

PACS numbers: 42.30.Wb; 87.63.L –; 87.64.Cc; 87.85.Pq
DOI: 10.1070/QE2008v038n06ABEH013850

Functional imaging and assessment of the glucose diffusion rate in epithelial tissues in optical coherence tomography

K.V. Larin, V.V. Tuchin

Abstract. **Functional imaging, monitoring and quantitative description of glucose diffusion in epithelial and underlying stromal tissues *in vivo* and controlling of the optical properties of tissues are extremely important for many biomedical applications including the development of noninvasive or minimally invasive glucose sensors as well as for therapy and diagnostics of various diseases, such as cancer, diabetic retinopathy, and glaucoma. Recent progress in the development of a noninvasive molecular diffusion biosensor based on optical coherence tomography (OCT) is described. The diffusion of glucose was studied in several epithelial tissues both *in vitro* and *in vivo*. Because OCT provides depth-resolved imaging of tissues with high in-depth resolution, the glucose diffusion is described not only as a function of time but also as a function of depth.**

Keywords: *glucose, permeability, noninvasive method, in-depth resolution, optical coherence tomography*.

1. Introduction

The development of noninvasive methods for functional imaging, monitoring, and assessment of glucose transport in epithelial tissues *in vivo* and the control of tissue optical properties are extremely important for many biomedical applications, including therapy, diagnostics, and improving the imaging of various devastating diseases such as cancer, arteriosclerosis, diabetes, and glaucoma. The successful management of these diseases requires long-term treatment with drugs. Unlike the traditional oral route, the use of topical and trans-dermal drug delivery by-passes first pass metabolism of the liver, the acidic environment of the gastrointestinal tract, and problems of pulsed absorption in the stomach. Topical drug delivery through skin and ocular tissues is currently recognised as a preferred route for drug administration.

Trans-dermal drug delivery is promising for drug administration because it is readily available, enables control of input, and excludes many problems associated with the oral or intravenous routes (such as drastic pH changes, the presence of enzymes, and rapidly fluctuating drug concentrations in plasma). However, only a limited number of drugs can be administered in this way due to the protective functions of skin. To improve permeability of skin, several penetration enhancers and specific procedures (e.g. heating and electrophoresis) can be applied [1 – 3]. Conventionally, *in vitro* methods have been used to assess the absorption of different drugs by skin [4]. The systematic *in vivo* study of trans-dermal drug delivery is required because the physical, physiological, and optical properties of living tissues can strongly differ from those of post mortem tissues [5].

Significant recent advances provided the optimisation drug delivery to target tissues within the eye for pharmacologic treatment and diagnostics of many ocular diseases [6]. Four main approaches are currently used to deliver drugs to different segments of the eye: systemic, intraocular, topical, and transscleral. The success of systemic administration is governed by the drug convective transport through blood vessels, diffusion across blood-vessel walls, and through tissues of the eye. For effective treatment, large systemic doses are required to overcome these rate-limiting barriers [7]. However, frequent administrations of drugs in large doses often cause severe systemic side effects. Furthermore, large macromolecular drugs (larger than 40 kDa and globular molecules larger than 70 kDa) are unable to diffuse through the internal limiting membrane of the retina [8, 9]. Therefore, the systemic drug delivery route is not practical in some cases and is rarely used for treatment of ocular diseases.

Intravitreal injections and intravitreal sustained-release implants provide the most direct approach for delivering therapeutic concentrations of drugs to eye tissues [10 – 12]. However, these approaches are essentially surgical procedures and require repeated injections. These invasive procedures frequently cause pain and have potential side effects of infection, retinal detachment, hemorrhage, endophthalmitis, and cataract. Topical drug delivery (TDD) through cornea and sclera of the eye is currently recognised as a preferred route for drug administration to treat many ocular diseases [13]. However, TDD is limited by the low permeability of the multilayered cornea and sclera, rapid clearance by tear drainage, and absorption into the

K.V. Larin Biomedical Optics Lab, Biomedical Engineering, University of Houston, 4800 Calhoun Rd., N207 Engineering Building 1, Houston, TX 77204, USA; Institute of Optics and Biophotonics, N.G. Chernyshevsky Saratov State University, ul. Astrakhanskaya 83, 410012 Saratov, Russia, e-mail: klarin@uh.edu;
V.V. Tuchin Institute of Optics and Biophotonics, N.G. Chernyshevsky Saratov State University, ul. Astrakhanskaya 83, 410012 Saratov, Russia; Institute for Problems of Precise Mechanics and Control, Russian Academy of Sciences, 410028 Saratov, Russia; e-mail: tuchin@sgu.ru

Received 13 February 2008; revision received 13 March 2008
Kvantovaya Elektronika **38** (6) 551 – 556 (2008)
Submitted in English

conjunctiva. Recent advances in the development of different TDD methods demonstrate improved ocular drug delivery by increasing drug contact time (e.g., by application of ointments, gels, liposome formulations, and various sustained and controlled-release substrates). The development of newer topical delivery systems using polymeric gels, colloidal systems, and cyclodextrins will provide exciting new therapeutics [14]. Therefore, more and more evidence suggests that corneal and transscleral TDD could be effective noninvasive methods for treatment of the eye disease and preferred ways of drug administration [13–18]. For example, human sclera has a high degree of hydration, a few proteins binding sites, and its permeability does not decline with age. Cornea and sclera are permeable to a wide range of solutes with different molecular sizes. All of these suggest that cornea and sclera are the ideal sites for the periocular drug delivery.

Controlling of tissue optical properties is another important application of drug (or clearing agent) delivery into epithelial tissues [5, 19]. The turbidity of biological tissues can be effectively controlled by using optical immersion methods based on the concept of matching refractive indices of scatterers and ground material. This technique proved useful in contrasting images of a living tissue and getting more precise structural, functional, and spectroscopic information from tissue depths otherwise inaccessible with different optical techniques [5, 19–23].

Recently, a new optical coherence tomography (OCT) method for noninvasive assessment of glucose in animal and human tissues has been developed [24–28]. This method is based on interferometric measurement and analysis of in-depth amplitude distribution of low-coherent light back-scattered from specific layers of tissues. The preliminary studies in animals and humans demonstrated that OCT is capable of sensitive and rapid assessment of changes in glucose concentration measured in interstitial fluid (ISF) of skin. However, insufficient accuracy, variability in measured lag time between changes of glucose concentrations in blood and ISF, fundamental difficulties with development of proper calibration algorithm, and problems with repeatability might limit its application in homes and clinics.

Early diagnostics is required for successful treatment and therapy of various epithelial disorders. Since many diseases alter structural organisation of tissues (e.g. by rearranging/modifying collagen organisation and, thus, directly affecting transport properties for molecules in these tissues) changes in diffusion or permeability of different chemical compounds and organic solutions, including biologically inert glucose molecules, may help develop a novel objective method for diagnosis of different tissue diseases and abnormalities.

In this paper we describe results on our recent efforts for the development of instrumentation based on OCT capable of real-time, sensitive, accurate, and noninvasive assessment of topical molecular diffusion in epithelial tissues that is of great scientific, clinical and pharmacological importance [29–32].

2. Materials and Methods

The experiments were performed by using a time-domain OCT system with a low-coherent broadband near-IR light source emitting 3 mW at 1310 ± 15 nm (Superlum Inc., Russia). The light beam scattered from a sample and the light beam reflected from the reference arm mirror formed an interferogram, which was detected with a photodiode. Two-dimensional images were obtained by scanning the incident beam over the sample surface in the lateral direction and in-depth (z-axial) scanning by the interferometer. The acquired images contained 450 by 450 pixels (2.2 by 2.4 mm). The full image acquisition time was approximately 3 s per image. The 2D images were averaged in the lateral direction (over $\sim$1 mm, that was sufficient for speckle-noise suppression) into a single curve to obtain an OCT signal that represented the in-depth 1D distribution of light in the logarithmic scale.

Ex vivo and *in vitro* experiments were performed with rabbit and monkey eyes and porcine skin and coronary artery. Pilot *in vivo* experiments were performed on monkey's skin. The experiments were performed within 24 hours after tissue nucleation. Tissues were kept cooled in a solution of appropriate physiological saline during transportation and storage. Right before *ex vivo* and *in vitro* experiments, the tissues were placed in a specially designed dish containing a physiological saline of normal room temperature. All experiments were performed at 22 °C. Continuous monitoring of tissue optical properties upon application of different molecules was performed for up to 2–2.5 hours. After experiments, the tissues were placed in $\sim$200 mL physiological solution and stored at +4 °C for 12–24 hours. The eye tissues were used in no more than two experiments while arteries and skin were used only once.

The permeability coefficients of glucose in tissues were calculated by using two different methods: OCT signal slope (OCTSS) and amplitude (OCTA) methods (Fig. 1). The OCTSS method was used to calculate the average permeability coefficient $\bar{P}$ of tissue stroma. The coefficient $\bar{P}$ was computed by dividing the thickness of the region used to calculate the OCTSS (typically, around 155–255 μm) by the time of agent diffusion inside this region $\bar{P} = z_{\mathrm{reg}}/t_{\mathrm{reg}}$. Since diffusion of glucose reflected in changes of the OCTSS and the signals were relatively constant before application of an agent and after saturation, t_{reg} was calculated as the time when the saturation stage was reached minus the time when the OCTSS started to change. The OCTA method of measurements was used to calculate the permeability coefficient at the specific depths in the tissues as $P(z) = z_{\mathrm{i}}/t_{z_{\mathrm{i}}}$, where z_{i} is the depth at which measurements were performed (calculated from the front surface) and $t_{z_{\mathrm{i}}}$ is the time of agent diffusion to this depth. The value of $t_{z_{\mathrm{i}}}$ was calculated from the time agent was added to the tissue until agent-induced change in the OCT amplitude was commenced. Note that unlike in OCTSS method, the value of z_{i} was calculated from epithelial surface of tissues to the specific depth in tissues' stroma in OCTA.

3. Results and discussion

Figure 2 shows typical results obtained for isolated rabbit sclera during water diffusion experiments. The OCT signal slope was calculated from the 279-μm region at a scleral depth of approximately 105 μm from the surface. A single application of a water droplet to the scleral surface was performed at the fifth min after the onset of the experiment. The propagation of water inside the sclera changed the local scattering coefficient and it was detected by OCT. The increase in local in-depth water concentration resulted in the decrease of the OCT signal slope during the hydration

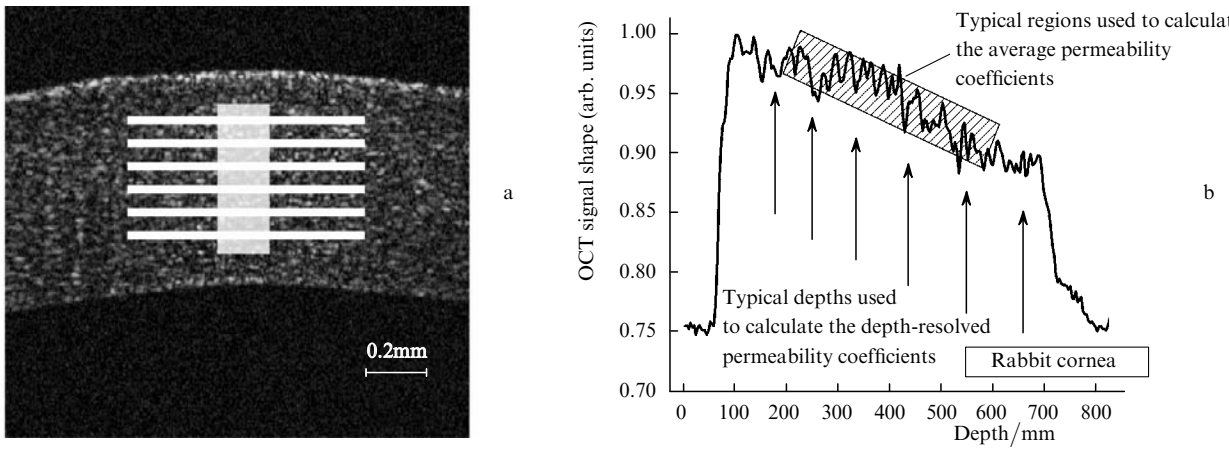

Figure 1. Scheme showing basic principles of two methods used to calculate molecular permeability coefficients: OCT Signal Slope (OCTSS) – calculating the average permeability coefficient in tissues' stroma and computed by dividing the thickness to the time – denoted by rectangles in (a) and (b); and OCT Amplitude (OCTA) – calculating permeability coefficient at different depths, thickness from epithelial layer to particular depth, time is computed from instant glucose was added until glucose-induced change in the OCT amplitude was commenced – denoted by bars in (a) and arrows in (b).

process and vice-versa during passive scleral dehydration (due to exposure of the sclera surface to air). The calculated water permeability rate, $\bar{P}^{w}_{isol}$, was approximately 6.6×10^{-5} cm s^{-1} in this experiment.

The OCT signal slope as a function of time recorded from cornea (partially submersed whole eyeballs experiments) during glucose diffusion experiment is shown in Fig. 3a. The OCT signal slopes were calculated from the 175-μm region at the corneal depth of approximately 350 μm from the epithelial surface. The permeability coefficient in this experiment was 1.62×10^{-5} cm s^{-1}. The OCT signal slope as a function of time recorded from sclera in fully submersed whole eyeballs experiments during glucose diffusion experiment are shown in Fig. 3b. The calculated glucose permeability coefficient was approximately 5.5×10^{-6} cm s^{-1}.

Fifty five experiments were performed with different sclera and 52 – with different rabbit cornea. Molecular permeability rates for the experiments with ocular tissues are described in [30]. These results correlates with coefficients published in earlier studies. For example, the permeability coefficient of ciprofloxacin in rabbit sclera was measured to be $(1.88 \pm 0.62) \times 10^{-5}$ cm s^{-1} [33]. Results for glucose diffusion are in a good correlation with results for human sclera [34].

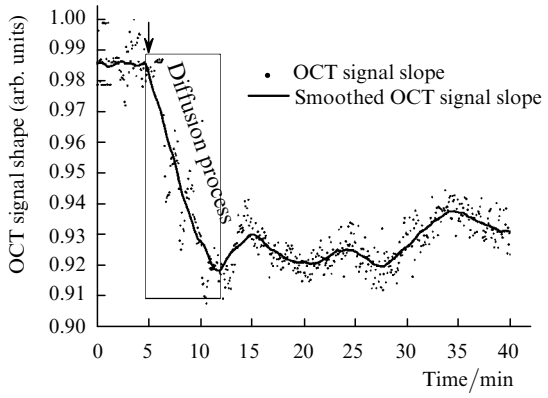

Figure 2. OCTSS as a function of time recorded from isolated sclera during water diffusion experiment. The arrow in this and all similar graphs indicates time of added agents. Smoothed OCTSS in this and all similar graphs was obtained by method of adjacent average of 20 neighbour data points (corresponding to approximately 1 min of experiment).

By comparing results from cornea and sclera, we can see that the permeability coefficients for the same molecules in the cornea and sclera are different. This discrepancy is likely due to the structural and physiological differences. Hydration is also considered a key factor in the study of permeability coefficients of agents through biological tissues. With hydration the fibrils move further apart creating extra space between them [35]. Swelling could come from the glycosaminoglycan (GAGs) or from anion bindings occurring in the tissue [36, 37]. The sclera has 10 times less GAGs than the cornea and the scleral stroma has a greater degree of fibrillar interweave than corneal stroma [38]. Thus, even though the cornea swells to many times its original weight in aqueous solution, the hydration of sclera increases only 20 % – 25 % [36]. It has been demonstrated that permeability coefficient is proportional to the tissues' hydration state. As the hydration in a tissue increases, the permeability coefficient increases as well [39].

Figure 3c shows a typical result from glucose diffusion studies in pig skin *in vitro*. The calculated permeability coefficient was approximately 8.95×10^{-6} cm s^{-1} in this experiment. Average glucose permeability in pig skin *in vitro* was $(7.69 \pm 0.56) \times 10^{-6}$ cm s^{-1} calculated from 5 independent experiments.

Pilot experiments were performed for glucose (20 %) diffusion experiments in rhesus monkeys (Macaca mulatta) skin *in vivo* (Figure 4). Even though typical skin layers of monkeys are thinner than that of human (e.g. thickness of epidermal skin layer is around 10 – 30 μm in monkeys and 50 – 100 μm in human), the anatomy and physiology are similar. All animal procedures were performed per protocol approved by University of Houston animal care committee. The animals were anesthetised according to the protocol. The animals were positioned and stabilised in a specially designed holder to restrict movements. OCT signals were

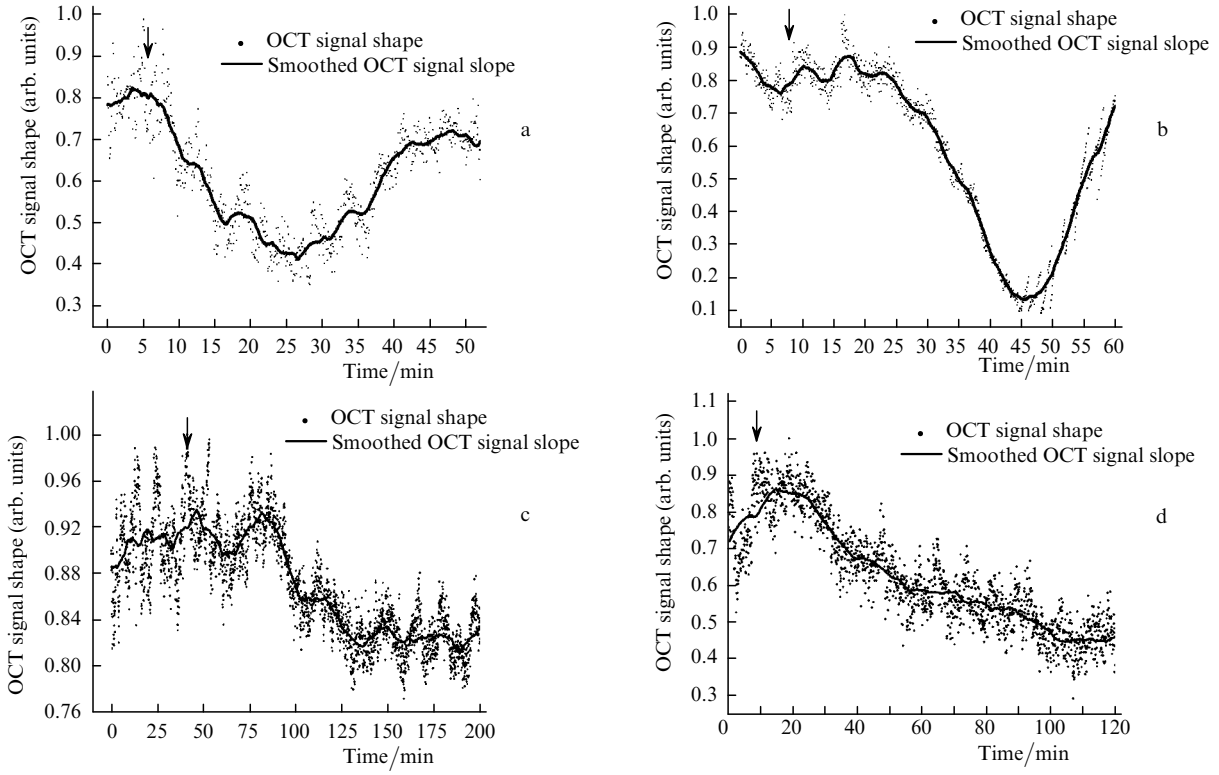

Figure 3. OCTSS as a function of time recorded from cornea in partially submersed whole eyeballs (a), in fully submersed whole eyeballs (b), from pig skin (*in vitro*) (c) and from monkey skin (*in vivo*) (d) during glucose diffusion experiment.

obtained from monkeys' skin at dorsal area. The area of OCT measurements was gently shaved and OCT probe was attached by using a special holder and taped (double-side tape) to the skin. An application of 20 % glucose solution (~ 1 mm^3) to the skin was performed at 10 – 15 min after onset of the experiment at the site of OCT imaging. In-depth changes of glucose concentration in skin were reflected in changes of the OCT signal slope (Fig. 3d). Calculated average glucose permeability from 5 independent experiments in skin *in vivo* was $(2.32 \pm 0.2) \times 10^{-6}$ cm s^{-1}.

Interesting results were obtained in measurements of glucose diffusion in healthy and arteriosclerotic pig aortas *in vitro*. Aortic tissues harvested from hypercholesterolemic pigs were surgically removed and experiments were conducted within 2 hours. The aortas were cut sagittally to create a sheet which was then cut to approximately 1-cm^2 square samples with and without arteriosclerosis. Figure 4a represents a typical OCTSS graph for a normal pig aorta during glucose diffusion experiment. The region monitored was about 75 μm in thickness and 280 μm away from the epithelial layer. The OCTSS decreased due to the reduction of scattering within the tissue caused by the local increase in the glucose concentration. Glucose solution reached the monitored region approximately 5 minutes after administration and took another 15 minutes for it to completely diffuse through. At that point, a reverse process in the OCTSS was shown. This change in the slope could be due to diffusion via concentration gradient differences on either side of the tissue; the net fluid (mainly water) movement from areas of high concentration to those of lower concentration would occur until equilibrium is reached. The permeability coefficient of glucose-20 % from 4 different

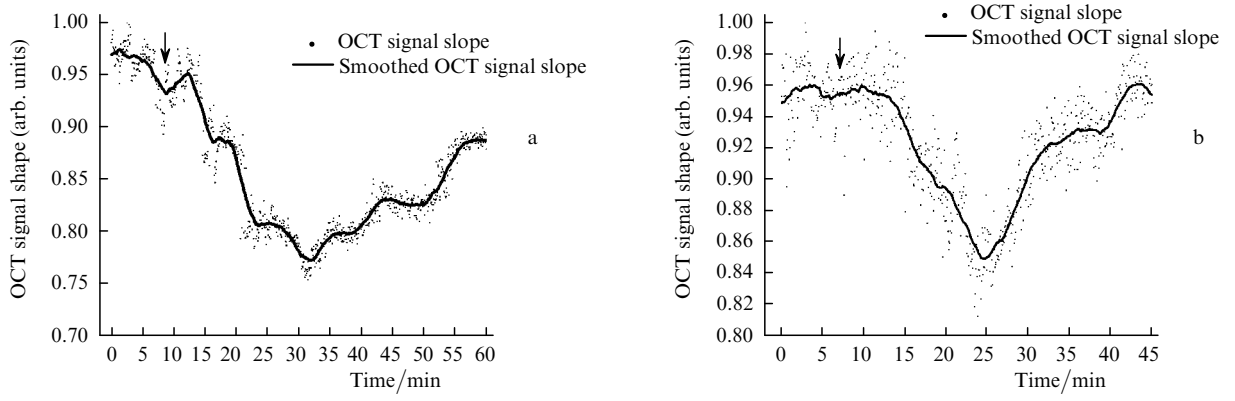

Figure 4. Typical OCTSS graph as a function of time recorded from a normal (a) and diseased (b) places of a pig aorta sample.

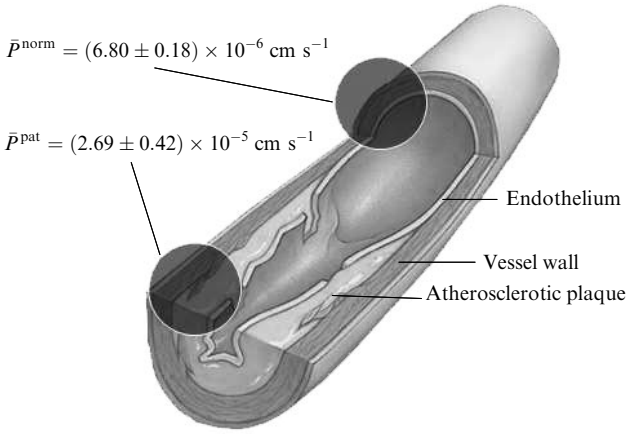

Figure 5. Glucose permeability coefficients measured in normal and diseased aorta samples.

experiments was found to be $(6.80 \pm 0.18) \times 10^{-6}$ cm s^{-1}. Figure 4b displays an atherosclerotic pig aorta tissue OCTSS graph during a glucose diffusion experiment. The same procedure was implemented as the normal tissues experiments. The specimen was imaged for about 7 minutes before glucose was added to the saline bath. The region selected in the diseased tissue was about 140 μm thick and 105 μm from the epithelial layer. The permeability coefficient of glucose-20 % in atherosclerotic aorta tissues was $(2.69 \pm 0.42) \times 10^{-5}$ cm s^{-1} ($n = 7$).

The results from this study indicate that atherosclerotic tissue had a higher permeability coefficient compared to that of healthy arterial regions (Fig. 5). These findings support the hypothesis that this OCT-based functional imaging method could measure glucose permeability coefficient as well as to distinguish normal and abnormal regions of the tissues.

The increased rate at which glucose diffused into the atherosclerotic tissue could be explained anatomically. Low-density lipoproteins (LDL) usually diffuse through the different layers of the aortic tissue to reenter circulation but at times can become trapped inside the intima. Inside the intima, the LDL's undergo oxidation and become modified. Macrophages migrate between the endothelial linings of the intima and start taking up the modified LDLs where they become engorged. This can lead to foam cell formation and eventually to an accumulation of plaque that protrudes into the lumen of the aorta. As the atherosclerotic plaque increases in size over time, the elastic tissues that form the aortic layers expand in order to compensate for the blockage and maintain adequate blood flow throughout the body. The expansion of the aorta could cause the numerous cells, fibers, and tissues of the aorta to readjust their organisation. From that organisational change, glucose could find the tissue easier to diffuse through. This expansion could explain the observed increase in the permeability coefficient of glucose with atherosclerotic tissue.

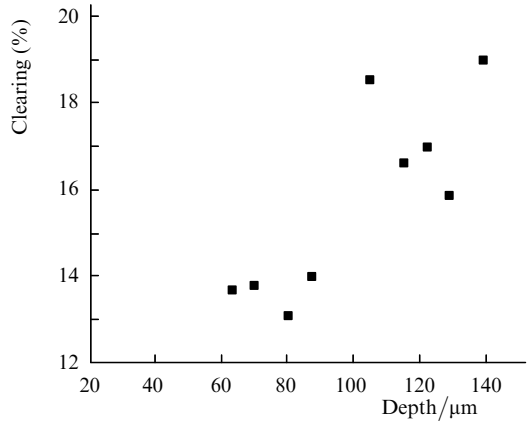

Figure 6. Optical clearing at different depth in a rabbit sclera.

OCT has many advantages over other popular imaging systems such as X-ray, MRI, and Ultrasound in terms of safety, cost, contrast, and resolution. However, lack of penetration depth into tissue is the main drawback of OCT. The turbidity of most biological tissues could prevent the ability of OCT to be fully engaged in various diagnostic and therapeutic procedures. In these experiments, we studied diffusion of glucose in tissues for its dual exploitation: depth-resolved quantification of its permeability as well as creating a 'clearer' medium which could assist in achieving higher depth penetration and, thus, enhancing diagnostic possibilities of light-based techniques.

The permeability coefficient of glucose was calculated in two different regions in the rabbit sclera: the upper 80–100 μm which constitutes a layer that includes the episclera and the following 100 μm region (which is thought to be in the stroma or the second layer). From five independent experiments, the permeability coefficient of glucose was found to be $(6.01 \pm 0.37) \times 10^{-6}$ cm s^{-1} in the upper region and $(2.84 \pm 0.68) \times 10^{-5}$ cm s^{-1} in the lower one. Additionally, the clearing effect of glucose on the sclera was computed using the OCT amplitude signal at different depths in the tissue during the diffusion process. The amplitude at a certain location inside the tissue was monitored during the diffusion process and the change in the light signal was observed; thus, the percent of optical clearing was calculated. The percentage of the clearing was estimated using the formula: $B = [(I_1 - I_2)/I_1] \times 100\,\%$; where I_1 and I_2 are the OCT signal amplitudes for the selected location before glucose started diffusing and after it had penetrated through, respectively. Figure 6 summarises the percent clearing of a rabbit sclera with glucose-40 % measured at different depths in the two selected regions. Roughly, the first 100 μm cleared around 10 % while the deeper 100-μm region cleared about 17 %–22% in these experiments.

4. Conclusions

Our experimental results have demonstrated the possibility of using OCT for measuring the permeability coefficient of glucose and its clearing effect in different layers of rabbit sclera. We have shown that deeper sclera layers are cleared better than external layers. The disparity in the collagen fibril sizes among the various layers in the sclera could have been the main reason for the dissimilarity in the clearing effect among different regions in the tissue. The structures of the different layers could have also been another source of differentiation in the optical clearing. The refractive index mismatch between the mitochondria, cytoplasm, cell membrane, extracellular media, and its components such as collagen and elastin fibers could be the major source of

scattering. The penetration of glucose in the episclera could have been mainly through the intracellular spaces; thus less glucose enters the cells and matches its organelles inside to the surrounding environment. The results for clearing in the rabbit stroma correlated well with previous studies.

The structural OCT images from our experiments did not allow effective differentiation of normal from diseased tissues. However, the functional images provided by the OCT enabled effective distinguishing of normal and abnormal tissue regions (Fig. 9). This information could significantly increase the specificity and accuracy of tissue classification and further OCT use in clinical imaging. It is possible that functional imaging using OCT could potentially differentiate even further the different components contained in advanced atherosclerotic lesions such as necrotic core and collagen.

Acknowledgements. The authors acknowledge the contribution of graduate and undergraduate students to the presented results, including Mohamad Ghosn, Steven Ivers, Natasha Befrui, Esteban Carbajal, and Narendran Sudheendran (University of Houston). The study was supported in part by grants from W. Coulter Foundation and Office of Naval Research (KVL), Federal Agency of Education of Russian Federation (1.4.06, RNP.2.1.1.4473), RFBR (N06-02-16740) and the Program of Innovative Universities of RF (VVT).

References

1. Jain A.K., Thomas N.S., Panchagnula R. *J. Controll. Release*, **79**, 93 (2002).
2. Stott P.W., Williams A.C., Barry B.W. *J. Controll. Release*, **41**, 215 (1996).
3. Schaefer H., Redelmeier T.E. *Skin Barier: Principles of Percutaneous Absorption* (Basel: Carger, 1996).
4. Kemppainen B.W., Reifenrath W.G. *Methods for Skin Absorption* (Boca Raton: CRC Press, 1990).
5. Tuchin V.V. *Tissue Optics: Light Scattering Methods and Instruments for Medical Diagnosis* (Bellingham, WA: SPIE Press, 2007).
6. Davis J.L., Gilger B.C., Robinson M.R. *Curr. Opin. Mol. Ther.*, **6**, 195 (2004).
7. Duvvuri S., Majumdar S., Mitra A.K. *Expert Opin. Biol. Ther.*, **3**, 45 (2003).
8. Kamei M., Misono K., Lewis H. *Am. J. Ophthalmol.*, **128**, 739 (1999).
9. Marmor M.F., Negi A., Maurice D.M. *Exp. Eye Res.*, **40**, 687 (1985).
10. Herrero-Vanrell R., Refojo M.F. *Adv. Drug Deliv. Rev.*, **52**, 5 (2001).
11. Jaffe G.J., Pearson P.A., Ashton P. *Retina*, **20**, 402 (2000).
12. Sanborn G.E., Anand R., Torti R.E., Nightingale S.D., Cal S.X., Yates B., Ashton P., Smith T. *Arch. Ophthalmol.*, **110**, 188 (1992).
13. Zhang W.S., Prausnitz M.R., Edwards A. *J. Controll. Release*, **99**, 241 (2004).
14. Le Bourlais C., Acar L., Zia H., Sado P.A., Needham T., Leverge R. *Progr. Retinal Eye Res.*, **17**, 33 (1998).
15. Ambati J., Gragoudas E.S., Miller J.W., You T.T., Miyamoto K., Delori F.C., Adamis A.P. *Invest. Ophthal. Vis. Sci.*, **41**, 1186 (2000).
16. Olsen T.W., Aaberg S.Y., Geroski D.H., Edelhauser H.F. *Am. J. Ophthalmology*, **125**, 237 (1998).
17. Grass G.M., Robinson J.R. *J. Pharmaceutical Sciences*, **77**, 3 (1988).
18. Lawrence M.S., Miller J.W. *Intern. Ophthalmology Clinics*, **44**, 53 (2004).
19. Tuchin V.V. *Optical Clearing of Tissues and Blood* (Bellingham, WA: SPIE Press, 2005) Vol. PM154.
20. Tuchin V.V., Maksimova I.L., Zimnyakov D.A., Kon I.L., Mavlutov A.H., Mishin A.A. *J. Biomed. Opt.*, **2**, 401 (1997).
21. Rylander C.G., Stumpp O.F., Milner T.E., Kemp N.J., Mendenhall J.M., Diller K.R., Welch A.J. *J. Biomed. Opt.*, **11**, 041117-1 (2006).
22. Larina I.V., Carbajal E.F., Tuchin V.V., Dickinson M.E., Larin K.V. *Laser Phys. Lett.*, **5**, 476 (2008).
23. Vargas G., Chan K.F., Thomsen S.L., Welch A.J. *Lasers Surg. Med.*, **29**, 213 (2001).
24. Esenaliev R.O., Larin K.V., Larina I.V., Motamedi M. *Opt. Lett.*, **26**, 992 (2001).
25. Larin K.V., Eledrisi M.S., Motamedi M., Esenaliev R.O. *Diabetes Care*, **25**, 2263 (2002).
26. Kholodnykh A.I., Petrova I.Y., Larin K.V., Motamedi M., Esenaliev R.O. *Appl. Opt.*, **42**, 3027 (2003).
27. Larin K.V., Motamedi M., Ashitkov T.V., Esenaliev R.O. *Phys. Med. Biol.*, **48**, 1371 (2003).
28. Larin K.V., Akkin T., Esenaliev R.O., Motamedi M., Milner T.E. *Appl. Opt.*, **43**, 3408 (2004).
29. Ghosn M., Tuchin V.V., Larin K.V. *Opt. Lett.*, **31**, 2314 (2006).
30. Ghosn M., Tuchin V.V., Larin K.V. *Invest. Ophthal. Vis. Sci.*, **48**, 2726 (2007).
31. Larin K.V., Ghosn M.G., Ivers S.N., Tellez A., Granada J.F. *Laser Phys. Lett.*, **4**, 312 (2007).
32. Larin K.V., Ghosn M. *Kvantovaya Elektron.*, **36**, 1083 (2006) [*Quantum Electron.*, **36**, 1083 (2006)].
33. Ke T.L., Cagle G., Schlech B., Lorenzetti O.J., Mattern J. *J. Ocul. Pharmacol. Ther.*, **17**, 555 (2001).
34. Bashkatov A.N., Genina E.A., Sinichkin Yu.P., Kochubei V.I., Lakodina N.A., Tuchin V.V. *Biofiz.*, **48**, 292 (2003).
35. Farrell R.A., McCally R.L. in *Principles and Practice of Ophthalmology* (Philadelphia, PA: Saunders, 1994).
36. Elliott G.F., Goodfellow J.M., Woolgar A.E. *J. Physiol.*, **298**, 453 (1980).
37. Hodson S., Kaila D., Hammond S., Rebello G., al-Omari Y. *J. Physiol.*, **450**, 89 (1992).
38. Maurice D.M. *The cornea and the sclera. In The Eye* (New York and London: Academic Press, 1969) Vol. 1.
39. Boubriak O.A., Urban J.P., Akhtar S., Meek K.M., Bron A.J. *Exp. Eye Res.*, **71**, 503 (2000).